Cyclic Nucleotide–gated Channels
Pore Topology Studied through the Accessibility of Reporter Cysteines

Andrea Becchetti, Katia Gamel, and Vincent Torre

From the Biophysics Sector, Scuola Internazionale Superiore di Studi Avanzati (SISSA), 30136, Trieste, Italy

abstract In voltage- and cyclic nucleotide–gated ion channels, the amino-acid loop that connects the S5 and S6 transmembrane domains, is a major component of the channel pore. It determines ion selectivity and participates in gating. In the α subunit of cyclic nucleotide–gated channels from bovine rod, the pore loop is formed by the residues R345–S371, here called R1-S27. These 24 residues were mutated one by one into a cysteine. Mutant channels were expressed in *Xenopus laevis* oocytes and currents were recorded from excised membrane patches. The accessibility of the substituted cysteines from both sides of the plasma membrane was tested with the thiol-specific reagents 2-aminoethyl methanethiosulfonate (MTSEA) and [2-(trimethylammonium)ethyl]methanethiosulfonate (MTSET). Residues V4C, T20C, and P22C were accessible to MTSET only from the external side of the plasma membrane, and to MTSEA from both sides of the plasma membrane. The effect of MTSEA applied to the inner side of T20C and P22C was prevented by adding 10 mM cysteine to the external side of the plasma membrane. W9C was accessible to MTSET from the internal side only. L7C residue was accessible to internal MTSET, but the inhibition was partial, ~50% when the MTS compound was applied in the absence of cGMP and 25% when it was applied in the presence of cGMP, suggesting that this residue is not located inside the pore lumen and that it changes its position during gating. Currents from T15C and T16C mutants were rapidly potentiated by intracellular MTSET. In T16C, a slower partial inhibition took place after the initial potentiation. Current from I17C progressively decayed in inside-out patches. The rundown was accelerated by inwardly applied MTSET. The accessibility results of MTSET indicate a well-defined topology of the channel pore in which residues between L7 and I17 are inwardly accessible, residue G18 and E19 form the narrowest section of the pore, and T20, P21, P22 and V4 are outwardly accessible.

key words: sulfhydryl reagents • MTS compounds • cysteine scanning mutagenesis • P loop • H5

introduction

Cyclic nucleotide–gated (CNG)[1] channels are partially homologous to *Shaker*-type voltage-gated K^+ channels (Kaupp et al., 1989; Jan and Jan, 1990; Kaupp, 1995). They have six membrane-spanning segments (Henn et al., 1995) and contain sequence motifs resembling the voltage-sensor (S4) and the pore-forming segment (P loop), which connects the S5 and S6 transmembrane domains (see Fig. 1). However, CNG channels typically require cyclic nucleotide to open, are only weakly voltage dependent in the presence of cyclic nucleotide, and are equally permeable to sodium and potassium ions (Baylor and Yau, 1989; Zagotta and Siegelbaum, 1996). A model of the pore loop topology is a necessary step towards understanding gating and permeation in CNG channels.

The substituted cysteine-accessibility method (SCAM; Akabas et al., 1992, 1994; Karlin and Akabas, 1998) has been widely used for studying the pore of voltage-dependent channels. In brief, amino-acid residues within the P loop are replaced in turn with cysteines; the accessibility of each mutated residue to different thiol-specific reagents is then tested. For this purpose, methanethiosulfonate (MTS) compounds have often been used. Strong current inhibition by MTS reagents is usually considered to be an indication that the tested cysteine lines the pore lumen. The main assumption is that charged, polar reagents react predominantly with thiols in the water-accessible surface (Stauffer and Karlin, 1994; Durell and Guy, 1996; Karlin and Akabas, 1998; Pascual and Karlin, 1998), the pattern of accessibility (from intra- or extracellular surfaces) gives information about pore topology.

In particular, 2-aminoethyl MTS (MTSEA) covalently links an ethylammonium group to the thiol of cysteines (Bruyce and Kenyon, 1982). Sun et al. (1996) found that several residues within the P region of CNG channels are accessible to MTSEA from both sides of the plasma membrane, in contrast with results obtained for voltage-gated potassium channels (Kurtz et al., 1995; Pascual et al., 1995a). This unexpected result suggested

Portions of this work have previously appeared in abstract form (Becchetti, A., K. Gamel, P. Roncaglia, and V. Torre. 1999. *Biophys. J.* 76:A7).

Address correspondence to Prof. Vincent Torre, Biophysics Sector, SISSA, Via Beirut 4, 30136 Trieste, Italy. Fax: 39-040-2240470; E-mail: torre@sissa.it

[1]*Abbreviations used in this paper:* CNG, cyclic nucleotide–gated; I/V, current–voltage; MTS, methanethiosulfonate; MTSEA, 2-aminoethyl MTS; MTSET, [2-(trimethylammonium)ethyl]MTS; SCAM, substituted cysteine-accessibility method; WT, wild type.

a model of the pore in which the P loops belonging to the four channel subunits are parallel to the membrane surface. In this way, many amino acid residues should be accessible to MTS compounds from both sides of the plasma membrane. In addition, some residues are differentially accessible in the open and closed states, an indication that, during gating, the P region should change its conformation considerably. MTSEA, however, although unable to permeate the open channel as a charged amine (Sun et al., 1996), readily crosses the lipid bilayer, probably because the uncharged amine is partially soluble into the plasma membrane (Holmgren et al., 1996; Wilson and Karlin, 1998). Thus, the accessibility to MTSEA of several P loop residues from the two sides of the membrane could be due to MTSEA permeation through the plasma membrane instead of being a consequence of the CNG channel topology. It is therefore important to assess the accessibility of some impermeant MTS derivatives, such as [2-(trimethylammonium)ethyl]MTS (MTSET; Stauffer and Karlin, 1994; Holmgren et al., 1996; Wilson and Karlin, 1998).

The P region of the α subunit of the CNG channel from bovine rod (Kaupp et al., 1989) is composed of the amino-acid residues R345 to S371 (here named R1–S27, see Fig. 1). In the absence of atomic-resolution structure, the accessibility pattern of the different residues inside the P region to different toxins, ions, and chemical probes is useful to propose structural models of the pore. Unfortunately, no specific toxins are known for CNG channels. Moreover, a large fraction of the cysteine mutants in the P region of CNG channels are not functional (Sun et al., 1996). In particular, no data are available on the accessibility of residues between Y8 and L14. The lack of experimental information about the structure of long stretches of amino acid residues is a serious impediment to the development of quantitative molecular modeling of permeation and gating (Durell et al., 1998) and to the performance of molecular dynamics simulations (Karplus and Petsko, 1990). It also prevents a thorough comparison between the pore structures of K^+ channels and CNG channels.

This paper has two purposes. First, to analyze the effects of MTSEA and MTSET applied to the inner and outer surface of patches containing different cysteine mutants in the P region of rod CNG channel. This allowed us to refine the assessment of the relative position of pore residues. Second, to test the accessibility of three residues not studied so far: two mutants within the Y8–L14 segment, namely W9C and L12C, and mutant P21C. Our results indicate a different accessibility for MTSEA and MTSET and suggest that the accessibility of several residues to MTSEA from both sides of the plasma membrane (Sun et al., 1996) is caused by MTSEA permeation through the lipid bilayer. MTSET effects suggest that the distinction between residues outwardly or inwardly accessible is clear cut, in the P loop of CNG channels, with an overall topology reminiscent of that of Kv2.1 voltage-dependent K^+ channels (Kurtz et al., 1995; Pascual et al., 1995a).

methods

Oocyte preparation. Wild-type and mutant channels were expressed in *Xenopus laevis* oocytes (purchased from H. Kahler, Institute fur Entwicklungsbiologie, Hamburg, Germany). Oocytes were extracted from frogs anesthetized with 0.2% tricaine methanesulfonate and treated as previously described (Nizzari et al., 1993). After injection, the eggs were incubated at 18°C in Barth's solution containing (mM): 88 NaCl, 1 KCl, 0.82 $MgSO_4$, 0.33 $Ca(NO_3)_2$, 0.41 $CaCl_2$, 2.4 $NaHCO_3$, 5 TRIS-HCl, pH 7.4, supplemented with 50 μg/ml gentamicin sulphate.

Currents were measured 2–5 d after mRNA injection, at room temperature (20–22°C). During the experiments, oocytes were maintained in Ringer solution containing (mM): 110 NaCl, 2.5 KCl, 1 $CaCl_2$, 1.6 $MgCl_2$, 10 HEPES, pH 7.4.

Molecular biology and mutant expression. The P region of the α subunit of the bovine rod CNG channel (Kaupp et al., 1989), spanning the amino acid residues R1–S27 (Fig. 1), was investigated using SCAM. The α subunit clone was mutated using the QuikChange™ Site-Directed Mutagenesis kit (Stratagene Inc.). All mutant RNAs were sequenced completely with the DNA sequencer LI-COR (4000L type). RNAs for wild-type (WT) and mutant channels were synthesized in vitro by using the mCAP™ RNA Capping kit (Stratagene Inc.). Functional channels were observed for mutants K2C, V4C, S6C, L7C, W9C, L12C, T15C, T16C, I17C, T20C, P21C, P22C, V24C, and S27C, with and without the background mutation C505T. No cGMP-activated current was measurable from mutants Y3C, Y5C, Y8C, S10C, T11C, L14C, E19C, or P23C. Some single-channel activity was found for mutants T13C and G18C, but the open probability was too low to allow reliable accessibility tests (Becchetti, A., and K. Gamel, manuscript submitted for publication). We did not study residues R1, R25, or D26.

Channel	1	3	5	7	9	11	13	15	17		19	21		23	25	27
Rod CNG	R	K	Y	V	Y	S	L	Y	W	S	T	L	T	L	T	T	I	G	-	-	E	T	P	P	-	P	V	R	D	S
Olf CNG		E	Y	I	Y	C	L	Y	W	S	T	L	T	L	T	T	I	G	-	-	E	T	P	P	-	P	V	K	D	E
Shaker		S	I	P	D	A	F	W	W	A	V	V	T	M	T	T	V	G	Y	G	D	M	T	-	-	P	V	G	F	W
Kv2.1	K	S	I	P	A	S	F	W	W	A	T	I	T	M	T	T	V	G	Y	G	D	I	Y	P	K					
KcsA		T	Y	P	R	A	L	W	W	S	V	E	T	A	T	T	V	G	Y	G	D	L	Y			P	V	T	L	W

Figure 1. Amino acid sequence alignment of the P loop residues in channels belonging to the voltage-gated ion channel superfamily (Jan and Jan, 1990). From top to bottom: sequence alignment of the a subunit of the bovine rod CNG channel (R345–S371, here numbered 1–27; Kaupp et al., 1989), the catfish olfactory CNG channel (E316–E341; Goulding et al., 1992), the Shaker voltage-gated K1 channel from Drosophila (S428–W454; Tempel et al., 1987), the Kv2.1 voltage-gated K1 channel from rat brain (K358–K382; Frech et al., 1989), and the KcsA K1 channel from Streptomyces lividans (KcsA, T61–W87; Schrempf et al., 1995).

Recording apparatus and data analysis. Currents from inside- and outside-out patches (Hamill et al., 1981) were recorded with a patch-clamp amplifier (Axopatch 200B; Axon Instruments Inc.). Borosilicate glass pipettes (Brand GmbH) had resistances of 2–5 MΩ, in symmetrical NaCl solutions. Patch currents were low-pass filtered at 10 kHz and stored on PCM\VCR. During the analysis, single-channel traces were low-pass filtered again at 2 kHz and sampled at 5 kHz (pClamp6 hardware and software; Axon Instruments). Macroscopic currents measured at constant membrane potential were digitized from PCM/VCR at 50 Hz. Currents for current–voltage relations were low-pass filtered at 1 kHz and acquired on-line (at 5 kHz) with pClamp6. The perfusion system was as previously described (Sesti et al., 1996).

Currents were analyzed with pClamp6 or SigmaPlot (Jandel Scientific). Data are usually given as mean ± SEM.

Accessibility to MTS Compounds from the Inner Side

Pipette contained (mM): 110 NaCl, 10 HEPES, 0.2 EDTA (standard solution, buffered with tetramethylammonium hydroxide, pH 7.6). Inside-out patches were perfused with the same solution supplemented, when necessary, with 0.5 mM cGMP and/or the appropriate MTS compound (2.5 mM). Current gated by cGMP was the difference between the currents in the presence and absence of cGMP. After allowing current and baseline stabilization, by applying cGMP several times, the MTS reagent was applied for 2–3 min. We followed the MTS effect continuously, at −40 mV, either in the presence (open state) or absence (closed state) of cGMP (Fig. 2, B and C). After washout, we measured the residual current for comparison with the initial current. At least once for each tested mutant, we also applied consecutive 200-ms voltage steps between −100 and +100 mV (20-mV increments; holding potential was 0 mV; Fig. 2), to study the current–voltage (I/V) relations before, during, and after MTS application. I/V relations potentially provide more information about mutant channel behavior during gating. When the current inhibition was irreversible, as expected for block due to covalent reaction of MTS with substituted cysteines, we perfused the inside face of the patch with Ringer solution. This procedure always activated oocyte's calcium-dependent chloride channels (Stühmer, 1992) and reassured us that the absence of a cGMP-activated current was not caused by the formation of a vesicle preventing the perfusion solution from reaching channels contained within the membrane patch. In the absence of MTS compounds, all mutants (except I17C) showed stable currents for at least 10 min (data not shown).

Accessibility to MTS Compounds from the Outer Side, in the Open State

The cGMP-activated current was measured from outside-out patches as the difference between the currents in the absence and presence of 5 mM external $MgCl_2$. Pipette (internal side) contained our standard solution supplemented with 0.5 mM cGMP, whereas $MgCl_2$ was added to the bath standard solution. Mg^{2+} ions completely block cGMP-gated currents from the extracellular side, at negative membrane potentials (Colamartino et al., 1991; Ildefonse and Bennett, 1991; Karpen et al., 1993; Root and MacKinnon, 1993; Sun et al., 1996). The effect of 5 mM $MgCl_2$ on the basal leak current (i.e., in the absence of cGMP) was negligible (data not shown). MTS compounds were applied for 2–3 min in the bath. The time course of their effect was usually followed at −40 mV. As for the intracellular experiments, whenever possible I/V relations were obtained before and after the effect of MTSET. In this case, however, membrane potential was stepped from −100 to +40 mV because the Mg^{2+} block is voltage dependent and complete only up to about +40 mV (Colamartino et al., 1991; Root and MacKinnon, 1993).

Accessibility to the MTS Compounds from the Outer Side, in the Closed State

We carried out inside-out experiments with MTSET in the pipette and, after measuring the initial current immediately after excision, followed the current kinetics at −40 mV by sampling the residual current with brief applications of cGMP (Sun et al., 1996). In these experiments, MTSET was constantly present on the outer side of the patch, from the moment of seal formation. Therefore, in mutants accessible from the outer side of the plasma membrane, we could follow the inhibition time course only when the procedure of seal formation and patch excision took ∼20–30 s. Otherwise, no cGMP-gated current was measurable in the presence of MTSET, even in patches excised from oocytes expressing high levels of CNG current (data not shown; see also Sun et al., 1996).

Materials. MTS reagents were purchased from Toronto Research Chemicals Inc. They were always dissolved in the appropriate solution at 2.5 mM before the experiment, and applied to the patch within ∼30 min. A relatively high concentration of MTS compounds is necessary when performing SCAM studies (Kurtz et al., 1995; Pascual et al., 1995a; Kuner et al., 1996; Sun et al., 1996; Wilson and Karlin, 1998), because the time course of the hydrolysis of thiosulfonates in saline solution at pH 7.6 is not known with precision (Karlin and Akabas, 1998). This time course, however, is similar for MTSEA and MTSET (Karlin and Akabas, 1998). Furthermore, control experiments performed on mutants sensitive to MTS compounds, like T20C and P22C, showed that in our experimental conditions MTSEA and MTSET were still completely effective 30 min after dissolvement (data not shown). All other chemicals were from Sigma Chemical Co.

results

In this paper, we describe results obtained with SCAM applied to the α subunit of the bovine rod channel (here called WT; Kaupp et al., 1989). When expressed in *Xenopus laevis* oocytes, WT channels form homomultimers (probably tetramers; Zagotta and Siegelbaum, 1996) with the main properties of native channels (Kaupp et al., 1989).

First, we show the effect of MTS compounds on WT channels (Fig. 2). Then we examine the accessibility of the different cysteine mutants to MTSEA and MTSET, from the outer and inner surface of excised membrane patches. Experiments were done at saturating concentrations of cGMP (0.5–1 mM; Becchetti and Gamel, 1999), in symmetrical NaCl, and in the absence of divalent cations. We will mostly show data obtained with MTSET, since our results with MTSEA agree with those reported by Sun et al. (1996).

Effect of MTS Reagents on Wild-Type Channel

MTSET (Fig 2. A) and MTSEA (not shown) produced a voltage-dependent block of WT channels, when applied to the patch inner side, in the presence of cGMP (i.e., when the channels were open). This block resembled the one caused by other organic cations (Picco and Menini, 1993). Since the channel inhibition at positive membrane potentials was reversible, the interaction of

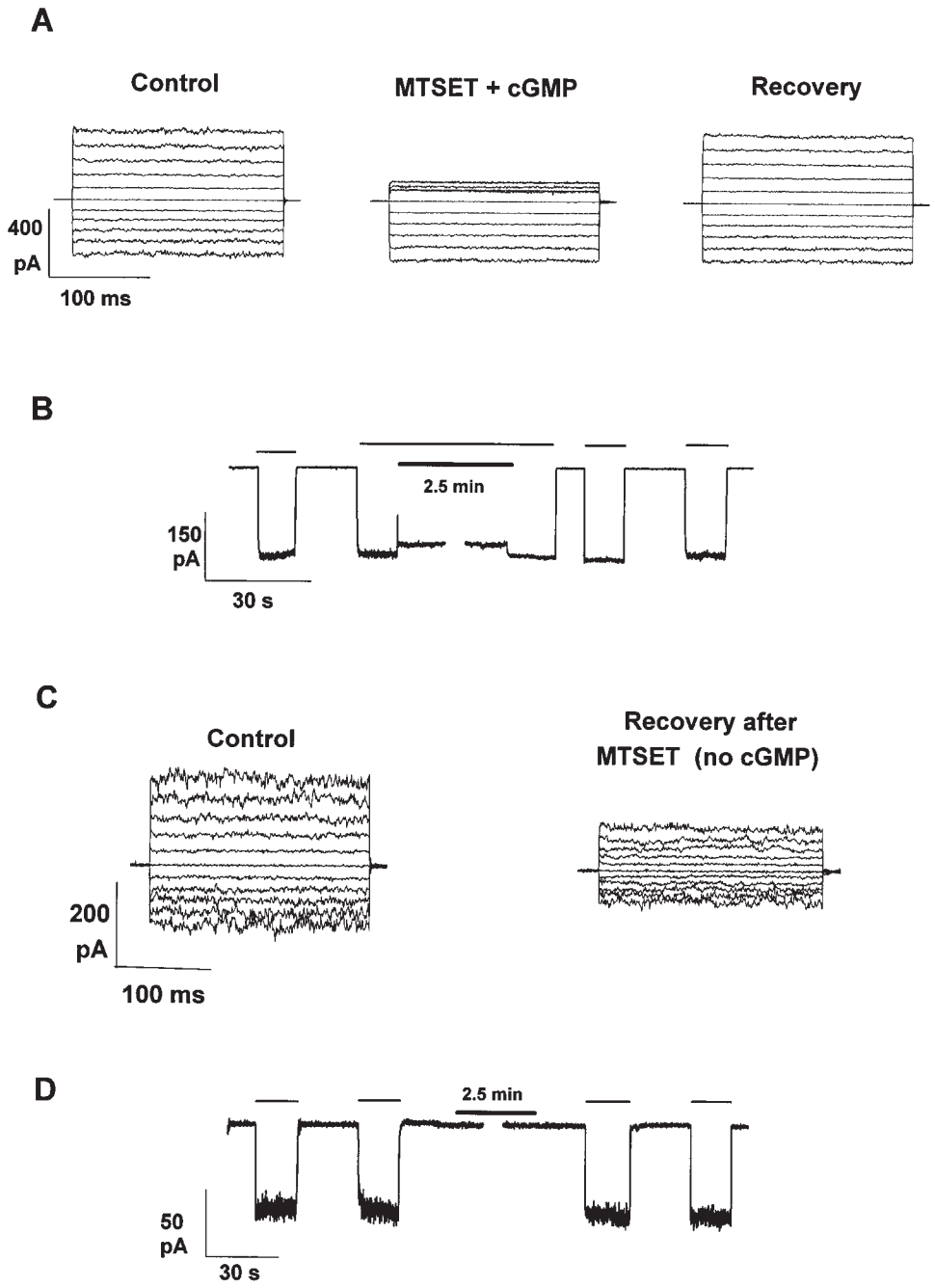

Figure 2. MTSET's effect on WT and C505T channels. (A) I/V relations from WT CNG channels, in inside-out patches, before (Control), during (MTSET + cGMP), and after (Recovery) application of 2.5 mM MTSET, in the presence of 500 μM cGMP (open state). Recovery was measured ~1 min after MTSET washout. Currents were elicited by 200-ms voltage steps from −100 to 100 mV (20-mV increments). Holding potential was 0 mV. Traces are averages of five trials. (B) MTSET had no irreversible effect on C505T channels in the open state. MTSET was applied for ~2.5 min at −40 mV in the presence of 500 μM cGMP. (C) MTSET irreversibly inhibited WT channels. I/V relations before (Control) and after (Recovery) application of 2.5 mM MTSET, in the absence of cGMP. (D) MTSET had no effect on C505T channels, in the closed state. MTSET was applied for ~2.5 min at −40 mV in the absence of cGMP. In Figs. 2–5 and 7–9, the thick bar indicates the duration of MTS application and the thin bar indicates either the application of 500 μM cGMP to the intracellular side of the membrane (for inside-out patches) or the time during which cGMP was present in the absence of Mg^{2+} (for outside-out patches). Unless otherwise indicated, membrane potential was always maintained at −40 mV.

MTS's with the open channel does not involve any covalent reaction with endogenous cysteines. On the contrary, when MTSET (Fig. 2 C) or MTSEA (not shown) were applied in the absence of cGMP (i.e., when the channels were closed), the subsequent perfusion of cGMP, after MTS reagent had been washed out, revealed a partial (~50%) irreversible current inhibition, independent of membrane potential. Sun et al. (1996) showed that MTSEA's irreversible block is removed by substituting the cysteine in position 505, within the cGMP-binding region, with a threonine. The same result applies to MTSET, which had no effect on C505T mutant channels either in the presence or absence of cGMP (Fig. 2, B and D). Therefore, when studying the MTS effect on CNG channels from the cytoplasmic side in the closed state, it is necessary to use cysteine mutants containing the supplementary mutation C505T. Fig. 2, B and D, also exemplifies our experimental procedure. Unless otherwise indicated, the MTS effect is shown for patches maintained at −40 mV. Usually, cGMP was applied two to three times before MTS application. The appropriate MTS reagent was then applied for 2–3 min. After washout, cGMP was applied again for comparison with the initial current (see methods).

Properties of Cysteine Mutants

The properties of cysteine mutants in the pore region were described in a previous paper (Becchetti and Gamel, 1999). In brief, no major difference was found between cysteine mutants and WT channels, in the affinity to cGMP and the selectivity to monovalent alkali cations. However, several cysteine mutants had altered gating compared with WT channels. Some of these effects will be commented upon below. The supplementary mutation C505T did not cause any effect in addition to preventing irreversible block by MTS compounds (data not shown).

Accessibility of K2C-L14C Residues

Neither MTSEA nor MTSET had any effect on mutants K2C and S6C (see Fig. 12). cGMP-activated currents from mutant V4C were not affected by MTSET application to the inner side of the plasma membrane, in either the closed or open state (Figs. 3 A and 12). On the contrary, MTSET strongly inhibited cGMP-gated currents in mutant V4C, when applied to the outer side of membrane patches, both in the presence and absence of cGMP (Figs. 3 B and 12). These results suggest that V4 is outwardly accessible and possibly located in the outer pore vestibule.

The segment formed by residues L7–L14 is very sensitive to cysteine mutation (Becchetti and Gamel, 1999), leading to mutant channels with a reduced maximal open probability and an altered gating. After RNA injection, functional channels were only measurable from L7C, W9C, and L12C mutants. cGMP-activated currents from L7C mutant were scarcely different from those observed in WT channels. They were not affected by external MTSET (Figs. 3 B and 12). However, MTSET application to the inner side of membrane patches produced a partial but reproducible block: 60% (±9.9%, n =

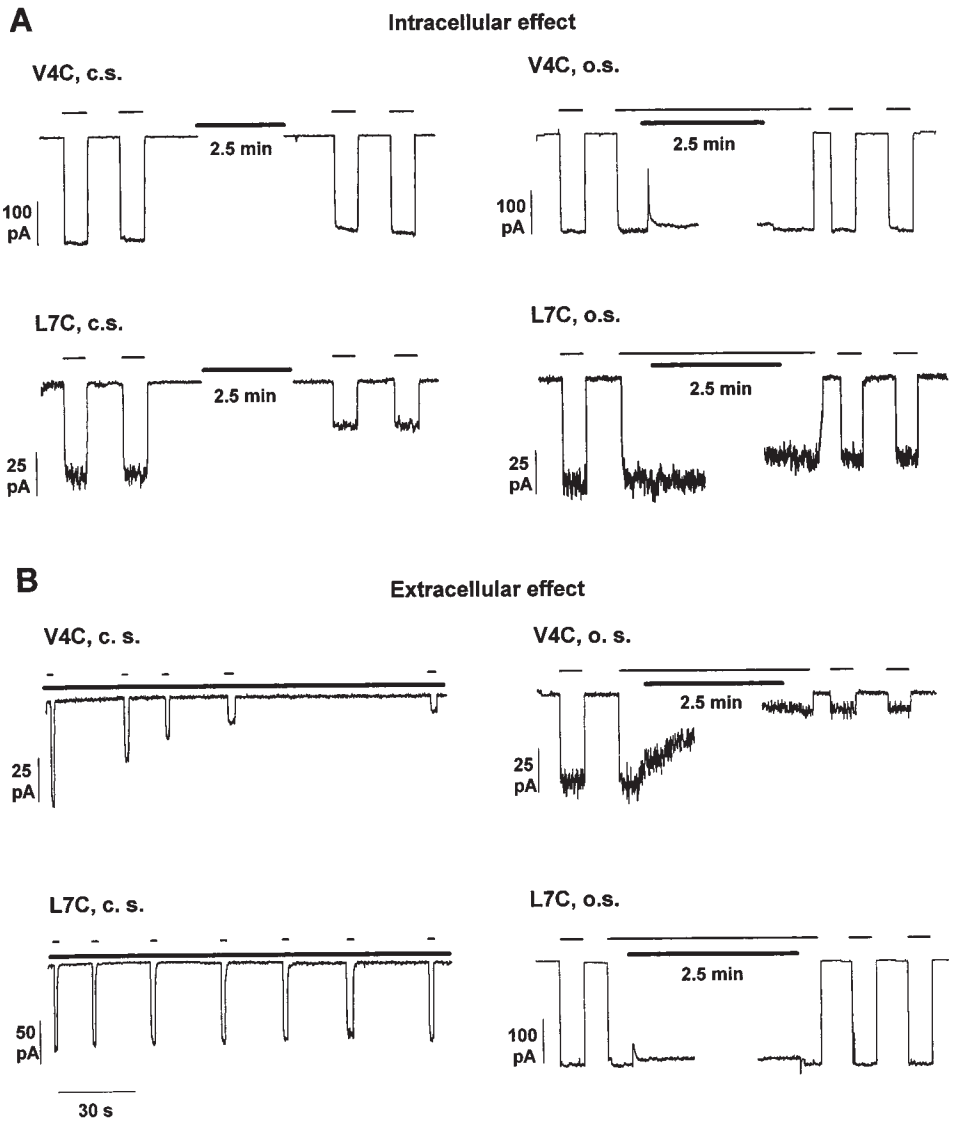

Figure 3. MTSET effect on V4C and L7C mutant channels. (A) MTSET application on the inner side of membrane patches. (Top) MTSET's effect on V4C mutant in the closed (c.s.) and open (o.s.) state. (Bottom) MTSET's effect on L7C mutant in the closed (c.s.) and open (o.s.) state. (B) MTSET application on the outer side of membrane patches. (Top) MTSET's effect on V4C mutant in the closed (c.s.) and open (o.s.) state. (Bottom) MTSET's effect on L7C mutant in the closed (c.s.) and open (o.s.) state.

4) in the closed state, and 25% (±3.6%, $n = 5$) in the open state (Fig. 3 A, bottom). These results show that L7 residue is accessible from the internal side of the plasma membrane. The difference between MTSET effect in the open and closed state is statistically significant ($P < 0.01$; Student's t test) and suggests that this residue changes its location during gating.

Mutant channels W9C and L12C had altered gating with outwardly rectifying I/V relations. In particular, W9C currents were consistently smaller than currents from the other mutant channels, due to low single-channel open probability at all membrane potentials (Becchetti and Gamel, 1999). External application of MTSET, in the presence of cGMP, had no effect on either mutant channel (Fig. 4 B). On the other hand, W9C mutant was inhibited, while L12C was potentiated by internal MTSET (Figs. 4 A and 12). These data indicate that cysteines introduced in positions 9 and 12 are accessible from the inner side of the plasma membrane.

The MTSET effect on the macroscopic W9C and L12C mutant currents (Fig. 4) could be due to an alteration of the single channel conductance and/or channel gating. To distinguish between these two possibilities, we applied MTSET to patches containing a limited number of CNG channels.

Fig. 5 A illustrates current recordings before (top) and after (bottom) MTSET application from a patch (representative of five experiments) containing at least two W9C mutant channels, at −80 mV. After treatment, the CNG channel activity decreased, and double openings appeared very rarely. The single-channel current amplitude before and after application of MTSET was ~2.1 pA, as shown in the amplitude histograms. Thus, MTSET did not alter the single-channel conductance of mutant W9C, but decreased its open probability.

Fig. 5 B illustrates a similar experiment (representative of three) performed with mutant channel L12C. In this case, the higher frequency of channel fluctuations made it difficult to resolve a clear peak in the amplitude histogram, corresponding to the open level (see also Becchetti and Gamel, 1999). However, no major change in the single-channel conductance was apparent from current traces and amplitude histogram, before (Fig. 5 B, top) and after (bottom) MTSET application, whereas the analysis of the amplitude histogram indicated a slight increase in the open probability after treatment, consistent with the small potentiation observed in macroscopic currents at the steady state (data not shown).

These data suggest that cysteines introduced in position 9 and possibly also in position 12 are inwardly accessible to MTSET.

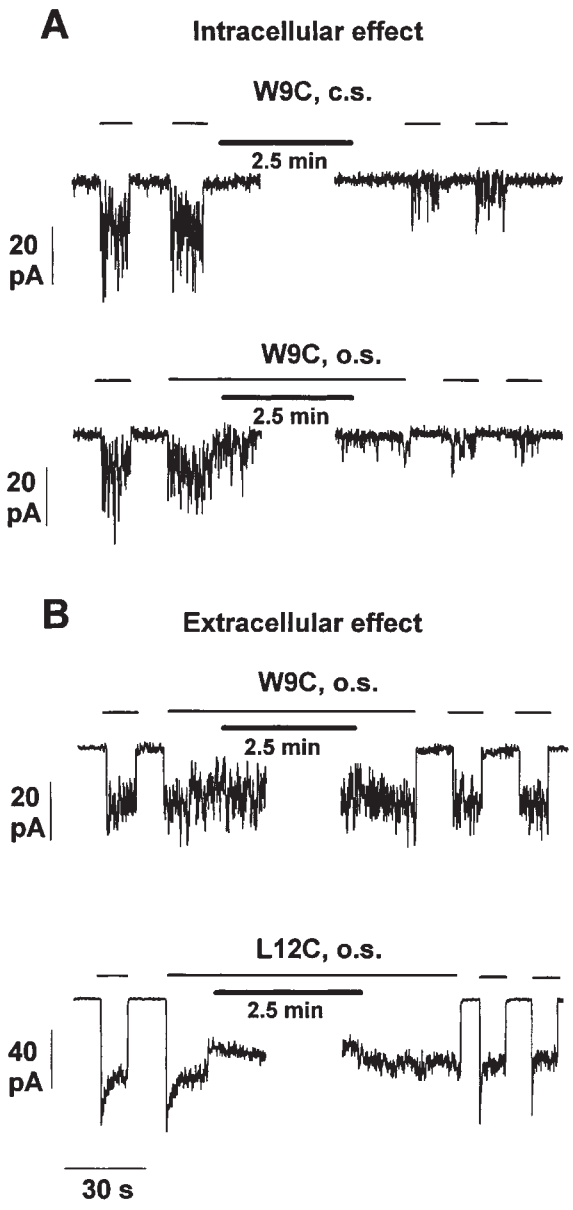

Figure 4. MTSET's effect on macroscopic currents from W9C and L12C channels. (A) MTSET application on the inner side of membrane patches. (Top) MTSET's effect on W9C mutant in the closed state (c.s.). (Bottom) MTSET's effect on W9C mutant in the open state (o.s.). (B) MTSET application on the outer side of membrane patches. (Top) MTSET's effect on W9C mutant in the open state (o.s.). (Bottom) MTSET's effect on L12C mutant in the open state (o.s.).

Accessibility of T15C and T16C Residues

Mutant channels T15C and T16C had similar properties (see Fig. 12); therefore, only data from T16C mutant will be presented. The cGMP-gated currents were strongly and rapidly potentiated by internal application of MTSET (and MTSEA, not shown), in the presence and absence of cGMP (Figs. 6, A and B, and 12). This potentiation varied from 50 to 200% and was almost absent when MTSET was applied from the outer side (Fig. 6 C). When MTSET was applied in the presence of cGMP, it was possible to follow the time course of its effect. After the initial fast potentia-

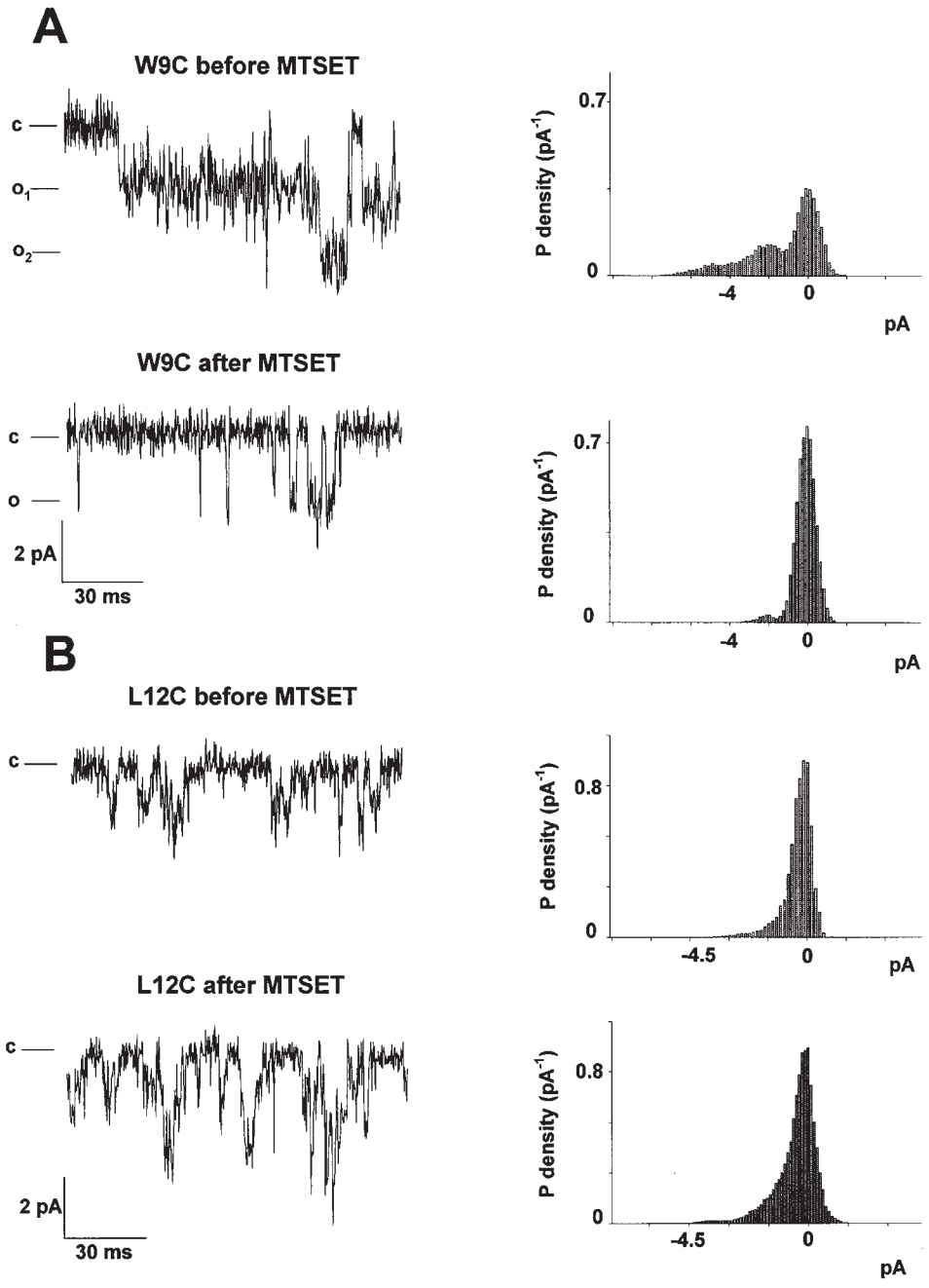

Figure 5. MTSET's effect on single-channel currents from W9C and L12C mutants. (A) W9C mutant single-channel traces before (top) and after (bottom) MTSET application to the inner side of the membrane patch, at −80 mV, in the presence of 1 mM cGMP. The amplitude histograms were obtained from ~10 s of continuous recording and reveal that at least two active channels were present in the patch. After MTSET application, the channel activity decreased considerably. This patch is representative of five experiments. (B) L12C mutant single-channel currents before (top) and after (bottom) MTSET application to the inner side of the membrane patch, at −100 mV, in the presence of 1 mM cGMP. In L12C, the increased frequency of channel fluctuations did not allow us to resolve a clear peak corresponding to the open state. However, the inspection of the current traces and amplitude histograms did not reveal any major change in channel conductance, whereas the lobe corresponding to the open state in the amplitude histogram became more populated, suggesting that the channel open probability increased after treatment.

tion, we observed a slow partial irreversible current inhibition reaching the steady state ~2 min after addition (Fig. 6). The partial inhibition with respect to the maximal current, measured shortly after MTSET addition, was 55% ± 8%. Fig. 10 (below) shows only the net steady state potentiation; i.e., the potentiation of the current measured after MTSET washout with respect to the current before treatment. It should be noted that the I/V relations of T16C mutant exhibited a weak inward rectification, and current traces revealed a time dependency in the development of the steady state current (Fig. 6 D, left). These features persisted after the MTSET effect (Fig. 6 D, right).

Moreover, we followed the potentiation in a patch containing a low number of channels (Fig. 7). Before MTSET application, single-channel recording at −60 mV in the presence of 0.5 mM cGMP exhibited only two distinct current levels, corresponding to the closed state and to an open state of 2.3 pA. After MTSET application, the open state became more populated and it was often possible to observe current openings of 4.6 pA, corresponding to the simultaneous opening of two channels. Thus, MTSET produced no major change in channel conductance, and the potentiation appears to be due to an increased open probability. A similar po-

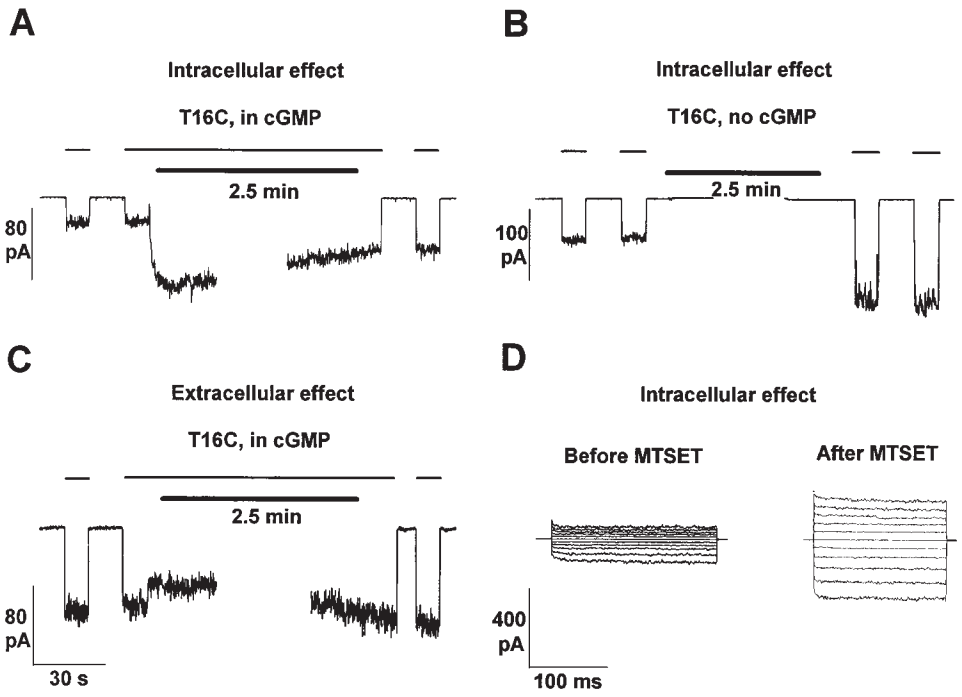

Figure 6. MTSET effect on T16C channels. (A) MTSET's effect on the inner side of membrane patches, in the presence of cGMP. (B) MTSET's effect on the inner side of membrane patches, in the absence of cGMP. (C) MTSET's effect on the outer side of membrane patches, in the presence of cGMP. (D) I/V relations before and after the application of MTSET on the inner side of membrane patches, in the absence of cGMP. Membrane potential was stepped from −100 to +100 mV (20-mV increments). Holding potential was 0 mV. Currents are the difference between the patch current in the presence and absence of cGMP. Current traces were the average of five consecutive trials.

tentiation was caused by MTSET application to the inner side of membrane patches containing T15C mutant channels. However, in this case, no inhibition followed the rapid initial potentiation (not shown). The potentiation produced by MTSET is a consequence of the low open probability of T15C and T16C channels, even in saturating cGMP (Fig. 7; Becchetti and Gamel, 1999). Furthermore, we investigated whether, in T15C, a partial inhibition produced by MTSET was masked by the strong potentiation. To assess this point, we perfused the inner side of patches containing T15C channels with our standard solution supplemented with 10 μM Ni^{2+} to activate maximally the channels within the patch (Gordon and Zagotta, 1995). After potentiation by nickel, MTSET did not produce any supplementary effect (data not shown).

On the other hand, MTSET application to the outer face of the plasma membrane produced negligible effects on both T15C and T16C mutants (Figs. 6 C and 12). These results suggest that residues in position 15 and 16 are not accessible from the extracellular side, and that T16C is accessible to MTSET from the inner side of the plasma membrane and may be partially involved in channel gating.

Accessibility of I17C Residue

Contrary to what was observed in all other cysteine mutants in the CNG channel pore, cGMP-activated currents recorded from the mutant channel I17C rapidly decayed in inside-out patches. Current did not recover even when patches were maintained several minutes in the absence of cGMP (data not shown). The current lifetime was prolonged by adding the reducing agent dithiothreitol to the medium bathing the inner side of the plasma membrane (Becchetti and Gamel, 1999). These results are reminiscent of those obtained in Na^+ channels, when mutants containing two substituted cysteines in the pore region are expressed in *Xenopus* oocytes (Benitah et al., 1997). As proposed for sodium channels, a possible explanation for these results is that cysteines in close proximity form disulfide bridges. In this view, cysteines in position 17 of neighboring subunits should be in closer contiguity than cysteines in the other functional mutants. The half-time ($t_{1/2}$) of the I17C current decay was 45.8 ± 5.2 s in the presence of 0.5 mM cGMP (Fig. 8 A, bottom) and 80.1 ± 12.1 s in the absence of cGMP (Fig. 8 A, top). The difference is statistically significant ($0.01 < P < 0.05$, Student's *t* test). Application of MTS compounds to the inner side of membrane patches strongly reduced the $t_{1/2}$ in the presence of cGMP, the average value being 20.4 ± 2.5 s (comparison with control value gave $P < 0.001$, from Student's *t* test; Fig. 8 B). The presence of MTS compounds also reduced the data scatter (Fig. 8 B). These results argue that residue in position 17 was inwardly accessible to our probe. We propose that I17 is located near the narrowest section of the channel pore, at its inward side (see discussion). The faster decay in the presence of cGMP suggests also that I17 residues of different subunits are closer to each other in the open state.

Accessibility of T20C–S27C Residues

Glutamate in position 19 is known to be accessible to both intra- and extracellular cations (Root and MacKin-

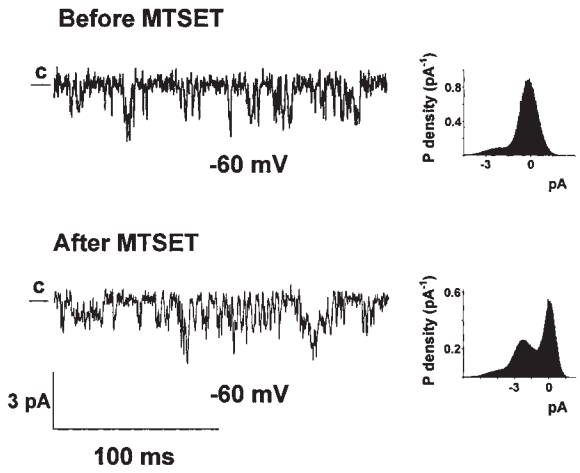

Figure 7. MTSET's effect on single T16C channels. (Top) Representative single channel traces before the application of MTSET (left) and corresponding amplitude histogram from 1 min continuous recording at −60 mV (right). (Bottom) Representative single channel traces after the application of MTSET to the inner side of membrane patches, in the absence of cGMP (left) and corresponding amplitude histogram from 1 min continuous recording at −60 mV (right). (c) Current level corresponding to the channel closed level.

non, 1993; Eismann et al., 1994; Sesti et al., 1995) and is believed to be close to the narrowest section of the channel pore (Sesti et al., 1995). When E19 was mutated to a cysteine, no functional channels were observed, thus the accessibility of this residue cannot be studied with SCAM. Therefore, it is particularly important to analyze the accessibility of residues in positions 20–22.

Both MTS reagents, when applied outwardly, strongly blocked T20C currents, both in the closed and open state (Figs. 9 B and 12). However, MTSEA and MTSET gave different results when applied to T20C channels from the inner side of the plasma membrane. MTSEA inhibited T20C current in both the open and closed state (see Figs. 10, B and C, and 12; see also Sun et al., 1996), whereas MTSET was not effective in either condition (Fig. 9 A). Similar results were found for P22C channels. In the latter however, at variance with WT and the other cysteine mutants, the reversible MTSET block was also present at negative membrane potentials. Furthermore, the inhibition of this mutant channel required a several-minute washout to be completely reversed. This suggests that the affinity of the channel pore for MTSET is increased in P22C mutant.

As shown in Figs. 9, 10, and 12, MTSEA applied to the inner and outer sides of membrane patches irreversibly inhibited T20C and P22C channels, while MTSET was only effective when applied to the external side. This suggests that the internal MTSEA inhibition, in these cases, is due to permeation of this compound through the lipid bilayer (Holmgren et al., 1996). To verify this possibility, we applied MTSEA to the inner side of inside-out patches containing either T20C or P22C, when the patch pipette contained 10 mM cys-

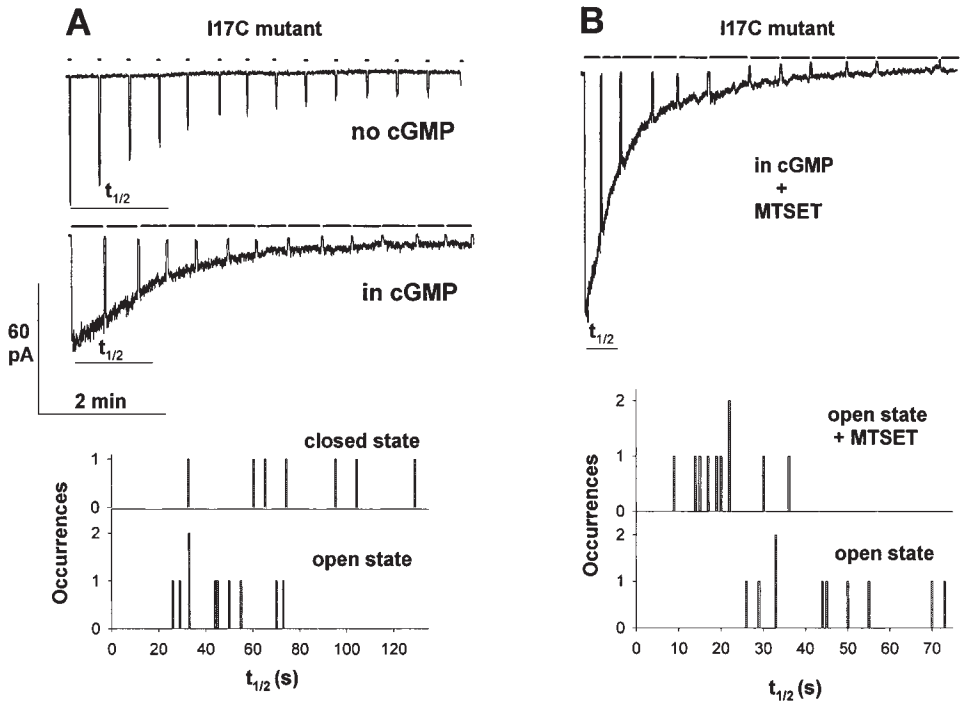

Figure 8. MTSET's effect on I17C mutant. (A) I17C current decay in inside-out membrane patches during continuous recording at −40 mV. (Top) Current rundown in the absence of cGMP. Residual current was sampled every 30 s by brief application of cGMP (short bars). (Middle) Current rundown in the presence of cGMP. Baseline level was checked every 30 s by briefly applying solution without cGMP. (Bottom) Current $t_{1/2}$ from 17 experiments in the absence (closed state) or presence (open state) of cGMP. Experimental procedure was as shown in top and middle panels. (B) I17C current decay in inside-out membrane patches during continuous recording at −40 mV in the presence of MTSET. (Top) Current rundown in the presence of cGMP. (Bottom) Current $t_{1/2}$ from 20 experiments in the presence of cGMP and MTSET (Open state + MTSET) and of cGMP in the absence of MTSET (open state).

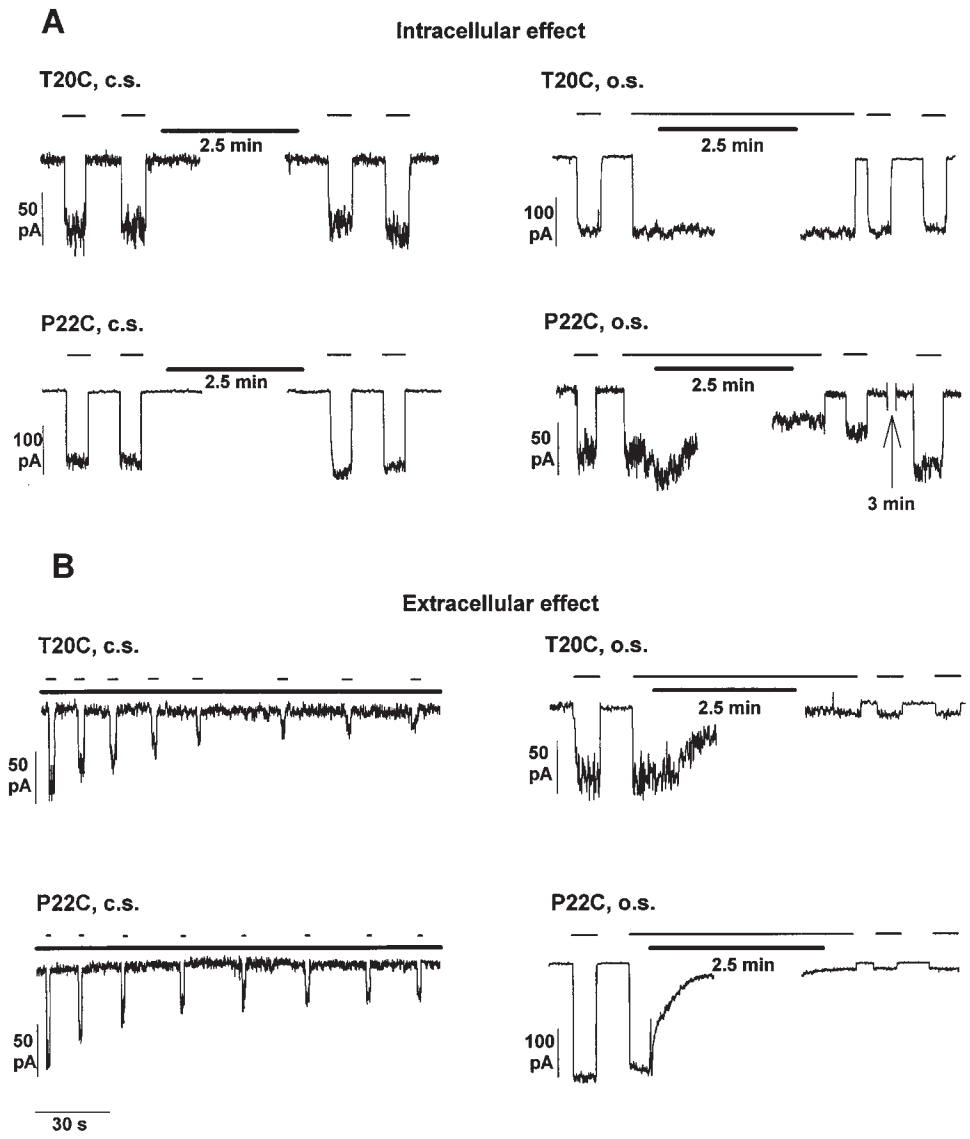

Figure 9. MTSET effect on T20C and P22C mutant channels. (A) MTSET application on the inner side of membrane patches. (Top) MTSET effect on T20C mutant in the closed (c.s.) and open (o.s.) state. (Bottom) MTSET effect on P22C mutant in the closed (c.s.) and open (o.s.) state. (B) MTSET application on the outer side of membrane patches. (Top) MTSET's effect on T20C mutant in the closed (c.s.) and open (o.s.) state. (Bottom) MTSET's effect on P22C mutant in the closed (c.s.) and open (o.s.) state.

teine, thereby used as a thiol scavenger on the outer side of inside-out patches (Holmgren et al., 1996; Wilson and Karlin, 1998). The presence of cysteine in the pipette solution did not affect the cGMP-gated current appreciably (Fig. 10 A).

In the presence of cysteine, the inhibition produced by MTSEA was always incomplete and partially reversible after washout (Fig. 10, B–D), although washout needed to be prolonged for several minutes, indicating again that cysteine mutation in residues T20 and P22 somewhat alters the channel affinity for MTS compounds. In the presence of external cysteine, MTSEA produced 48% ± 8.6% block on T20C channels ($n = 6$), and 23% ± 12% block on P22C channels ($n = 3$), whereas the inhibition in the absence of cysteine was always complete and irreversible even after 10–15-min washout for both mutants. In this case, we have pooled experiments in which MTSEA was applied in the presence and absence of cGMP, since no difference was found between the two conditions. Cysteine rescue of MTSEA internal block on T20C and P22C currents reinforces the conclusion that T20 and P22 are outwardly accessible.

The effect of MTS compounds on mutants T20C and P22C was also studied at a single-channel level. Fig. 11 shows current traces from a patch probably containing two active P22C mutant channels, before (top) and after (bottom) MTSEA application to the inner side of the plasma membrane. Currents were recorded at −100 mV, in the presence of 1 mM cGMP.

After treatment, no openings were observed and the amplitude histograms of current fluctuations in the presence and absence of cGMP became identical. This result is consistent with MTSEA causing a complete channel block and suggests that the residue in position 22 lines the permeation pathway. Similar results were obtained with T20C mutant (data not shown).

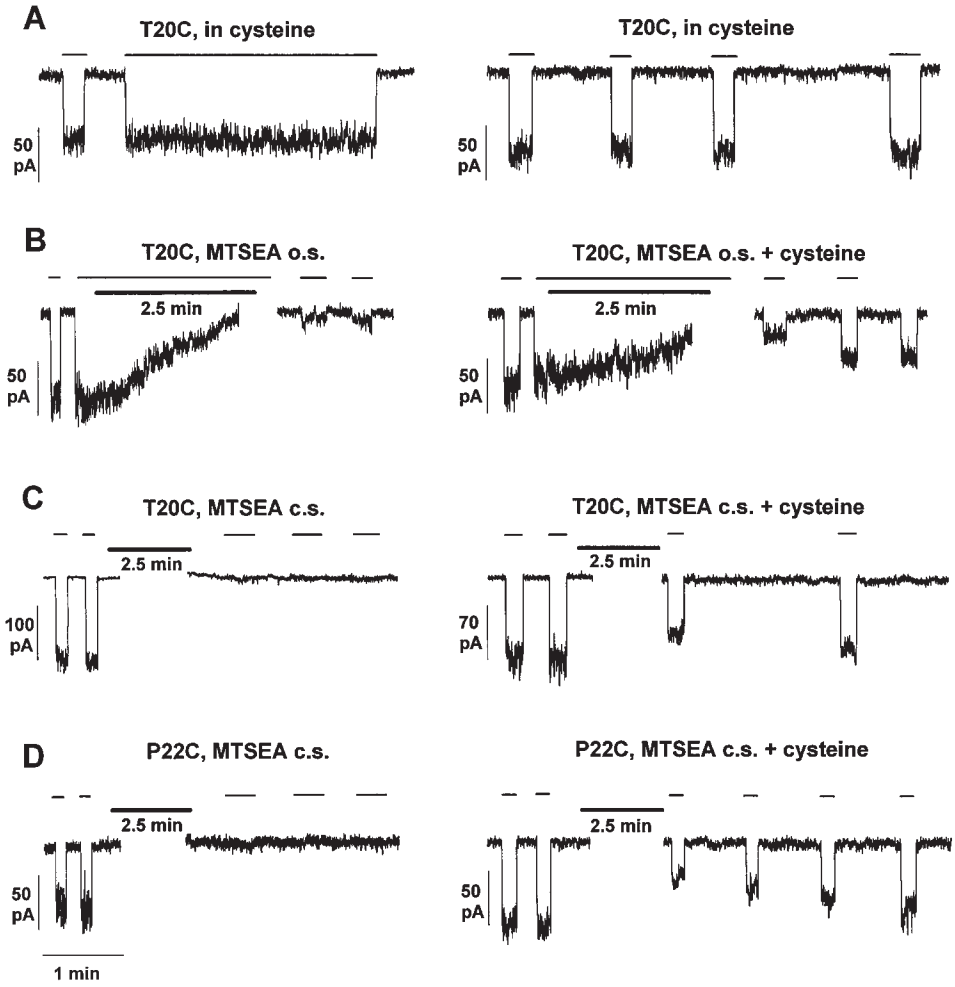

Figure 10. Cysteine prevented MTSEA effect on T20C and P22C channels. (A) 10 mM cysteine applied to the outer side of membrane patches had no effect on T20C currents. (Left) Cysteine applied in the open state. (Right) Cysteine applied in the absence of cGMP. (B) Effect of MTSEA applied to the inner side of patches containing T20C channels in the open state (o.s.). (Left) MTSEA irreversibly inhibited T20C current. (Right) 10 mM cysteine on the outer side of the patch prevented the irreversible block produced by MTSEA applied to the patch inner side. (C) Effect of MTSEA applied to the inner side of patches containing T20C channels in the closed state (c.s.). (Left) MTSEA irreversibly inhibited T20C current. (Right) 10 mM cysteine on the outer side of the patch prevented the irreversible block produced by MTSEA applied to the patch inner side. (D) Effect of MTSEA applied to the inner side of patches containing P22C channels in the closed state (c.s.). (Left) MTSEA irreversibly inhibited P22C current. (Right) 10 mM cysteine on the outer side of the patch prevented the irreversible block produced by MTSEA applied to the patch inner side.

Finally, inwardly applied MTSET had no effect on P21C currents, whereas it produced a small block (~25%, Fig. 12) when applied externally. Negligible effects were produced by MTSET on V24C and S27C mutant channels (Fig. 12). We conclude that T20, P21, and P22 are outwardly accessible residues. The weak effect on P21C indicates that the side chain of this residue does not line the channel pore lumen, after cysteine mutation at least.

discussion

The results presented in this paper show that several amino acid residues in the P loop of the rod CNG channel are differently accessible to MTSEA and MTSET. The accessibility map of the residues tested with MTSET (Fig. 12) is consistent with a topological structure of the pore region different from the one previously proposed (Sun et al., 1996), and more similar to that of voltage-dependent K^+ channels (Lu and Miller, 1995; Kurtz et al., 1995; Pascual et al., 1995a,b; Durell and Guy, 1996; Gross and MacKinnon, 1996; Doyle et al., 1998; Durell et al., 1998), which have a significant homology with CNG channels (Fig. 1). Due to the experimental variability (see, e.g., Karpen et al., 1993), we assumed that only average MTSET effects >20% inhibition or potentiation provided information on residue accessibility (Fig. 12).

Comparison with Previous Work

Our results obtained with MTSEA (in the absence of cysteine on the trans side) are broadly in agreement with those reported by Sun et al. (1996), but some differences have been found that merit a brief discussion. Our single-channel recordings show that mutant channels with a cysteine in the pore loop often had a low maximal open probability (Figs. 5 and 7; see also Becchetti and Gamel, 1999). Hence, the difference in MTS compounds accessibility in the "closed" and "open" states (i.e., in the absence or presence of a saturating cGMP concentration) must be interpreted with some caution, especially regarding the cysteine mutants within the segment W8-I17, which show the strongest alterations in the open probability. The cGMP-gated current rundown we observed when recording from

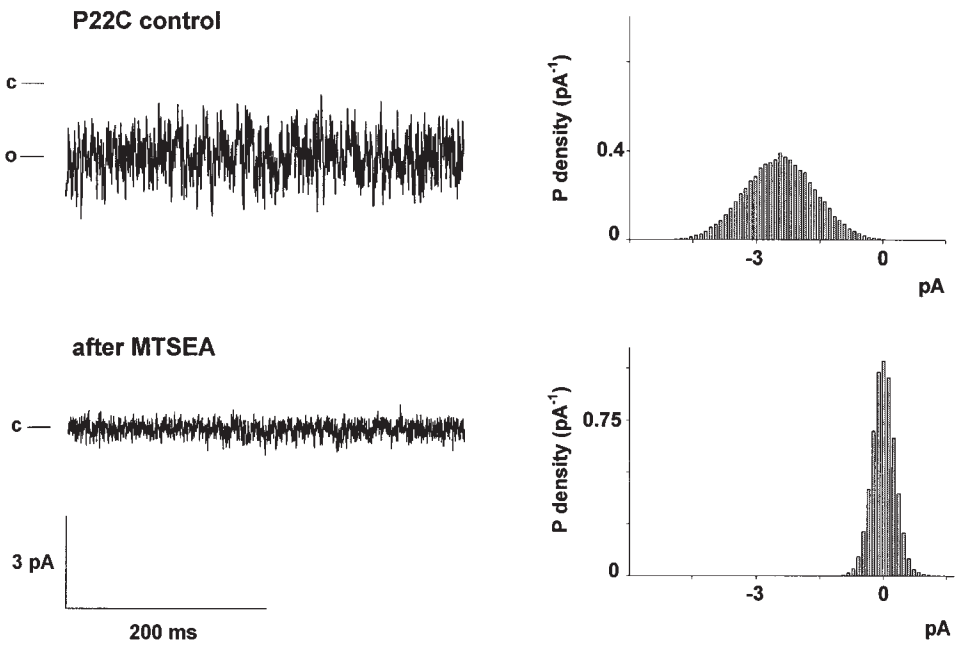

Figure 11. MTSEA's effect on P22C single-channel currents. (Top) P22C single-channel traces before MTSEA application to the inner side of the membrane patch at −100 mV in the presence of 1 mM cGMP. (Bottom) Current recording after treatment with MTSEA. The amplitude histograms were obtained from ~10 s of continuous recording and show that channel activity decreased drastically after MTSEA application. The amplitude histograms obtained after treatment were identical irrespective of whether cGMP was present or not, whereas cGMP application before treatment stimulated the typical intense "noisy" CNG channel activity reflected in the wide amplitude histogram, with a peak around −2.2 pA. This patch is representative of three experiments.

I17C mutant channels (see Fig. 8) was not reported by Sun et al. (1996). A possible explanation for this discrepancy is that these authors have always applied MTSEA after current had reached the steady state, which would explain the very low I17C current amplitude they observed. Finally, the initial MTS-induced potentiation we observed in T15C and T16C mutant channels is larger than that described by Sun et al. (1996). Again, if Sun et al. (1996) have plotted the steady state MTSEA effect, there is no contrast between our data and theirs; the slow incomplete block we have observed in T16C mutant, following the quick potentiation, agrees with the data reported by them. Despite this general agreement, our topological model for the pore, described in the last section below, differs from that of Sun et al. (1996). The reason for this disagreement is that we base our model on the results we obtained with MTSET inwardly or outwardly applied and on the results we obtained with MTSEA applied inwardly, in the presence of cysteine on the external side (where MTSEA should react only with residues accessible from the inner side).

Outwardly Accessible Residues: Comparison between MTSEA and MTSET Effect

The MTSEA and MTSET effects on cysteine mutant channels were different from one another. MTSEA targets several residues when applied from either side of the plasma membrane (Sun et al., 1996; Fig. 10). In contrast, we found that residues V4C, T20C, P22C, and (to a lesser extent) P21C were only accessible to outwardly applied MTSET. Furthermore, cysteine on the outer side of the patch prevented MTSEA block from the inner side (Fig. 10). We conclude that these differences arise because MTSEA, but not MTSET, is partly permeant through the plasma membrane as a charged amine (Holmgren et al., 1996; Wilson and Karlin, 1998), and propose that V4, T20, P21, and P22 are only accessible from the outer side of the membrane. Glutamate in position 19 is located at (or near) the narrowest region of the pore (Root and MacKinnon, 1993; Eismann et al., 1994; Sesti et al., 1995; Fodor et al., 1997). Therefore, T20, P21, and P22 are likely to form the outer pore vestibule, in agreement with the strong current inhibition produced by external MTSET on T20C and P22C mutants. The block produced by MTSET applied to the outer side of V4C mutant channels suggests that V4, too, is an outwardly accessible residue (Fig. 3). Data are consistent both with a location of V4 within the extracellular pore vestibule and with a possible crucial involvement of V4 in the gating process, not necessarily involving the channel vestibule.

Residues I17–E19

Current activated by cGMP from I17C mutant spontaneously decayed in inside-out patches (Fig. 8). This decay is slowed down by inwardly applied dithiotreithol (Becchetti and Gamel, 1999), suggesting that current rundown is due to the formation of disulfide bridges in excised patches. It is likely that the formation of disulfide bridges is prevented inside the intact oocyte, because of the reducing intracellular environment (Creighton, 1993). As shown in Fig. 8, the MTS compounds

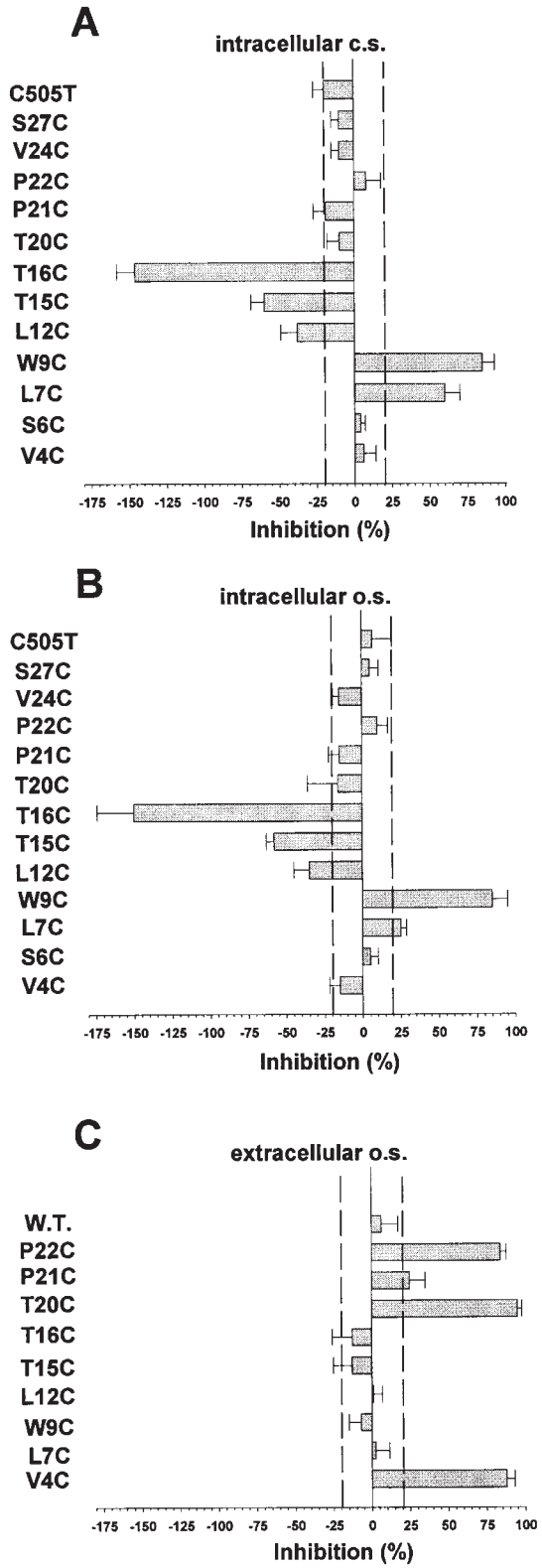

Figure 12. Summary of MTSET effects on mutant channels on the indicated mutants. (A) Intracellular MTSET effect in the absence of cGMP. (B) Intracellular MTSET effect in the presence of cGMP. (C) Extracellular MTSET effect in the presence of cGMP. The experimental procedure was explained in Fig. 3. The dashed lines mark the 20% level of inhibition or potentiation, which we considered significant for inferences about residue accessibility (see text).

decreased the half time of current decay, when applied to the inner side of membrane patches. The time course of current rundown was slower in the absence of cGMP, suggesting that this residue may move slightly towards the pore axis during channel opening. These results suggest that I17C residue is inwardly accessible. In addition, when the adjacent residues G18 and E19 were replaced by a cysteine, no functional channels were observed. In this case also, the lack of expression may be due to the formation of disulfide bridges, since E19 residue is thought to line the channel pore. This residue is accessible to extracellular divalent cations (Root and MacKinnon, 1993; Eismann et al., 1994) and to monovalent cations applied to the inner side (Sesti et al., 1995), and is a strong determinant of CNG channel permeation (Root and MacKinnon, 1993; Eismann et al., 1994; Sesti et al., 1995). Hence, we suggest that I17 residue faces the inner side of the plasma membrane and is located within the channel pore, and that G18 and E19 form the narrowest section of the pore itself.

Inwardly Accessible Residues

Within the segment L7-T16, only mutants L7C, W9C, L12C, T15C, and T16C produced functional channels in *Xenopus* oocytes. None of these mutants was affected by external MTSET, whereas all were sensitive to inward application of MTSET, though to different degrees. cGMP-gated currents from L7C and W9C were inhibited, indicating directly that residues L7C and W9C are accessible from the intracellular side. On the contrary, currents from L12C, T15C, and T16C were potentiated. It should be noted that, in all of these mutants, single-channel recording showed a decrease in open probability with respect to the WT channels in saturating cGMP (Figs. 5 and 7; Becchetti and Gamel, 1999). Therefore, we cannot exclude that cysteine substitution of these residues makes cGMP a partial agonist, analogous to what was found after mutating E19 (Bucossi et al., 1997; Zagotta and Siegelbaum, 1996). In this case, the potentiation exerted by intracellular MTSET may be caused by an aspecific interaction between the cationic MTSET and channel portions different from the substituted cysteine, as, for instance, the residue H420, responsible for cGMP-gated current potentiation, at submaximal cGMP concentrations (Gordon and Zagotta, 1995). However, since intracellular MTSET had a partial irreversible inhibitory effect on T16C after the quick initial potentiation, and the residues L7, W9, and I17, which bracket the L12–T16 segment, were inhibited by intracellular

treatment, we suggest that L12, T15, and T16 face the inner side of the plasma membrane.

Structural Model of the Pore Loop

In light of the results presented and discussed in this manuscript, the model shown in Fig. 13 is proposed for the pore loop topology in CNG channels. Residues accessible to MTSET from the external side of the plasma membrane were colored in red, residues accessible from the internal side were colored in blue, and white residues were either not accessible to MTS compounds or were not studied because cysteine substitution on these positions did not yield functional channels. The arrows indicate suggested displacements occurring during channel opening. Residues I17, G18, and E19 form the narrowest portion of the pore, whereas residues T20, P21, P22, and P23 form the extracellular channel vestibule. The three prolines 21–23 may form a polyproline loop (Creighton, 1993). The diameter of the extracellular vestibule lumen, lined by residues T20, P21, and P22, is likely to be wider than the diameter of the pore lumen at the level of the residues G18–E19 for two reasons. First, the large thiol reagent MTSET can readily reach all these residues. Second, in mutant channels T20C, P21C, and P22C, cysteines of neighboring subunits are not likely to become so close to each other to form disulfide bonds, leading to channel occlusion. In fact, macroscopic cGMP-gated currents from mutants T20C, P21C, and P22C, in symmetrical sodium and in saturating cGMP, usually have amplitudes comparable with those of WT currents, with no evidence of rundown (data not shown; Becchetti and Gamel, 1999). Residue G18 may cause a turn in the P loop so that only the adjacent I17 residues belonging to the different subunits are still sufficiently close to form disulfide bridges, when substituted with cysteines, whereas the following residues towards the amino terminal do not line the pore lumen.

Residues in the segment from L7 to T16 are intracellular. In particular, residues L7 to T13 have a significant homology, with residues L66 to T72 forming the final portion of the pore outer helix in KcsA potassium channel (Doyle et al., 1998). Therefore, residues L7 to T13 in CNG channels may form an alpha helix. Residues from L7 to V4 span the plasma membrane and residue V4 is extracellular, possibly being part of the outer pore vestibule. It should be recalled here that the residues that form the segment 321–339, towards the amino terminal with respect to V4, were shown to be extracellular by immunocytochemistry (Wolfhart et al., 1992).

Our model of the CNG channel pore differs from that of Sun et al. (1996) because we have not observed any substituted cysteines in the P loop to be accessible by MTSET from both sides of the plasma membrane. The difference in the two models reflects the fact that MTSEA can cross the lipid bilayer (Holmgren at al., 1996) and thus react with residues inaccessible to MTSET (or MTSEA in the presence of cysteine on the trans side).

Structural Changes during Channel Gating

The accessibility to MTSET of most of the tested residues was similar irrespective of whether MTSET was applied in the presence or absence of cGMP. In mutants whose open probabilities were 0.8 or larger, in saturating cGMP (as is also the case for WT channels), the presence or absence of cGMP was a tool to study the accessibility in the open or closed state, respectively. In

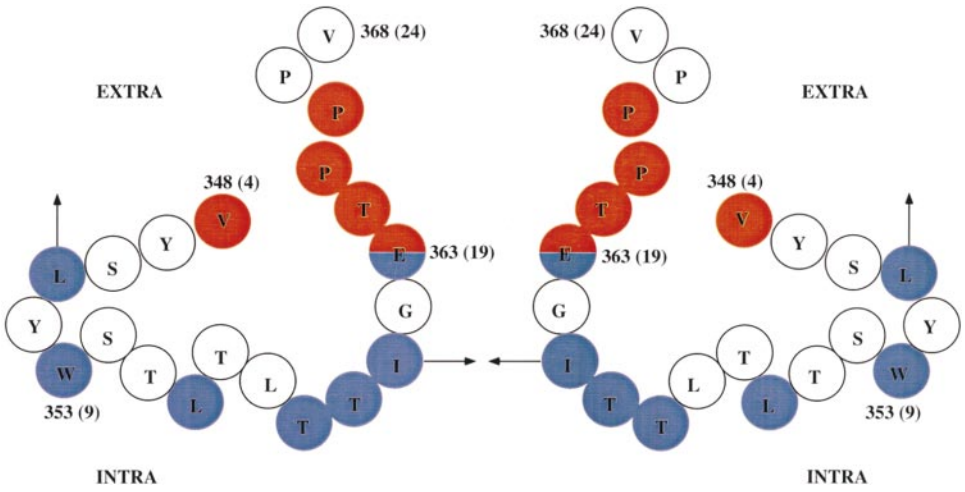

Figure 13. Model of the proposed topology of two adjacent P loops in CNG channels. Arrows indicate the suggested displacements occurring during channel opening. Red circles represent proposed extracellular residues. Blue circles represent proposed intracellular residues. White circles represent residues not accessible to MTS compounds or residues which, when substituted with cysteine, prevented the expression of functional channels. Residues are numbered according to their position in the CNG channel protein (Kaupp et al., 1989). The residue position corresponding to the conventional numbering R1–S27 used in this paper is given within brackets. (Extra) Extracellular side, (Intra) intracellular side.

mutants whose open probabilities were smaller (all mutants between W9C and T16C; Becchetti and Gamel, 1999), the distinction between accessibility in the open and closed state was not clear-cut, since even in the presence of saturating cGMP the channels remained in the closed state for a considerable fraction of the time. MTSET inhibition of L7C channels (Fig. 3) was slightly larger in the closed state, suggesting that, in the open state, L7 residue either moves towards the extracellular side of the plasma membrane or becomes less accessible. On the contrary, the accessibilities of residues T20, P21, and P22 were almost identical in the closed and open state, indicating that the outer vestibule does not undergo any large conformational rearrangement during gating. The faster rundown of cGMP-activated current in mutant I17C in the open state (Fig. 8) may be taken as an indication that residues I17 are closer to each other in the open than in the closed state. These results suggest, but do not prove, that the opening of the CNG channel is primarily mediated by a widening of the channel lumen near residues 18 and 19, which is accompanied by a movement of I17 residues towards the pore axis. This is in agreement with reports that residue E19 is accessible to internal tetracaine in the closed but not open configuration (Fodor et al., 1997).

Comparison to the Pore Loop of Voltage-dependent Potassium Channels

The comparison between the SCAM data presented here and the pore structure of the voltage-dependent K^+ channels presents both similarities and differences. SCAM has been applied to the study of the pore loop topology of voltage-dependent Kv2.1 delayed rectifying channels from rat brain (Kurtz et al., 1995; Pascual et al., 1995a). In Kv2.1 channels, the MTSET effects identify two distinct pore loop segments whose residues are accessible from either the outer or the inner side of the plasma membrane. In particular, residues D378 to K382, corresponding to G18–P22 in CNG channels (Fig. 1), were outwardly accessible (Kurtz et al., 1995; Pascual et al., 1995a,b). On the other hand, residues T370 to V374, corresponding to T13–I17 in CNG channels, were mostly accessible to MTSET applied inwardly (Pascual et al., 1995a,b). Furthermore, residue P361 in Kv2.1 channels, corresponding to V4 in CNG channels, was accessible to extracellular MTSET and Cd^{2+}, whereas residues A362–T372, corresponding to Y5–T15 in CNG channels, were not affected by external MTSET and Cd^{2+} (Kurtz et al., 1995). In contrast, in their studies of the *Shaker* K^+ channels, Lu and Miller (1995), using Ag^+, and Gross and MacKinnon (1996), using MTSEA, found only outwardly accessible sites, with the periodicity of an α helix, within the segment D431–V438, consistent with the atomic resolution KcsA channel structure (Doyle et al., 1998). These residues correspond to Y5–L12 in CNG channels (Fig. 1), among which we found only inwardly accessible residues (L7, W9, and possibly L12). Therefore, K^+ and CNG channels share some structural homology in the pore region, but they also show significant differences in the first part of the P segment, even though, in this area, their amino acid sequences are very similar (Fig 1).

We thank Prof. K.-W. Yau for reading and commenting on the manuscript. Thanks are also due to Mr. Claudio Becciani for invaluable technical support, to Mrs. Paola Roncaglia and Ms. Giada Pastore for preparing some of the mutant RNAs, and to Dr. Anna Rosati for help in sequencing. Miss L. Giovanelli kindly checked the English.

This study was funded by the European Community Biotechnology Project TRANS PL 960593.

Submitted: 12 April 1999 Revised: 23 June 1999 Accepted: 24 June 1999

references

Akabas, M.H., D.A. Stauffer, M. Xu, and A. Karlin. 1992. Acetylcholine receptor channel structure probed in cysteine-substitution mutants. *Science.* 258:307–310.

Akabas, M.H., C. Kauffmann, P. Archdeacon, and A. Karlin. 1994. Identification of acetylcholine receptor channel-lining residues in the entire M2 segment of the alpha subunit. *Neuron.* 13:919–927.

Baylor, D., and K.-W. Yau. 1989. Cyclic GMP-activated conductance of retinal photoreceptor cells. *Annu. Rev. Neurosci.* 12:289–327.

Becchetti, A., and K. Gamel. 1999. The properties of cysteine mutants in the pore region of cyclic nucleotide-gated channels. Pflügers Arch. In press.

Benitah, J.P., R. Ranjan, T. Yamagishi, M. Janecki, G.F. Tomaselli, and E. Marban. 1997. Molecular motions within the pore of voltage-dependent sodium channels. *Biophys. J.* 73:603–613.

Bruice, T.W., and G.L. Kenyon. 1982. Novel alkyl alkanethiosulfonate sulfhydryl reagents. Modification of derivatives of l-cysteine. *J. Protein Chem.* 1:47–58.

Bucossi, G., M. Nizzari, and V. Torre. 1997. Single-channel properties of ionic channels gated by cyclic nucleotides. *Biophys. J.* 72: 1165–1181.

Colamartino, G., A. Menini, and V. Torre. 1991. Blockage and permeation of divalent cations through the cyclic GMP-activated channel from tiger salamander retinal rods. *J. Physiol.* 440:189–206.

Creighton, T.E. 1993. Proteins. Structures and Molecular Properties. 2nd ed. W.H. Freeman and Co., New York. NY. 507 pp.

Doyle, D.A., J.M. Cabral, R.A. Pfuetzner, A. Kuo, J.M. Gulbis, S.L. Cohen, B.T. Chait, and R. MacKinnon. 1998. The structure of the potassium channel: molecular basis of K^+ conduction and selectivity. *Science.* 280:69–77.

Durell, S.R., Y. Hao, and H.R. Guy. 1998. Structural models of the transmembrane region of voltage-gated and other K^+ channels in open, closed and inactivated conformations. *J. Struct. Biol.* 121: 263–284.

Durell, S.R., and H.R. Guy. 1996. Structural model of the outer vestibule and selectivity filter of the *Shaker* voltage-gated K^+ channel. *Neuropharmacology.* 35:761–773.

Eismann, E., F. Muller, S.H. Heinemann, and U.B. Kaupp. 1994. A single negative charge within the pore region of a cGMP-gated channel controls rectification, Ca^{2+} blockage, and ionic selectivity. *Proc. Natl. Acad. Sci. USA.* 91:1109–1113.

Fodor, A.A., K.D. Black, and W. Zagotta. 1997. Tetracaine reports a conformational change in the pore of cyclic nucleotide–gated channels. *J. Gen. Physiol.* 110:591–600.

Frech, G.C., A.M.J. VanDongen, G. Schuster, A.M. Brown, and R.H. Joho. 1989. A novel potassium channel with delayed rectifier properties isolated from rat brain by expression cloning. *Nature.* 340:642–645.

Gordon, S.E., and W.N. Zagotta. 1995. A histidine residue associated with the gate of the cyclic nucleotide–activated channels in rod photoreceptors. *Neuron.* 14:177–183.

Goulding, E.H., J. Ngai, R.H. Kramer, S. Colicos, R. Axel, S.A. Siegelbaum, and A. Chess. 1992. Molecular cloning and single-channel properties of the cyclic-nucleotide–gated channel from catfish olfactory neurons. *Neuron.* 8:45–58.

Gross, A., and R. MacKinnon. 1996. Agitoxin footprinting the *Shaker* potassium channel pore. *Neuron.* 16:399–406.

Hamill, O.P., A. Marty, E. Neher, B. Sakmann, and F.J. Sigworth. 1981. Improved patch-clamp technique for high resolution current recording from cells and cell-free membrane patches. *Pflügers Arch.* 391:85–100.

Henn, D.K., A. Baumann, and U.B. Kaupp. 1995. Probing the transmembrane topology of cyclic nucleotide–gated ion channels with a gene fusion approach. *Proc. Natl. Acad. Sci. USA.* 92:7425–7429.

Holmgren, M., Y. Liu, Y. Xu, and G. Yellen. 1996. On the use of thiol-modifying agents to determine channel topology. *Neuropharmacology.* 35:797–804.

Ildefonse, M., and N. Bennett. 1991. Single-channel study of the cGMP-dependent conductance of retinal rods from incorporation of native vesicles into planar lipid bilayers *J. Membr. Biol.* 123: 133–147.

Jan, L.Y., and Y.N. Jan. 1990. A superfamily of ion channels. *Nature.* 345:672.

Karlin, A., and M.H. Akabas. 1998. Substituted-cysteine-accessibility method. *In* Methods in Enzymology. Vol. 293. P.M. Conn, editor. Academic Press, Inc., San Diego, CA. 123–136.

Karpen, J.W., R.L. Brown, L. Stryer, and D.A. Baylor. 1993. Interactions between divalent cations and the gating machinery of cyclic GMP–activated channels in salamander retinal rods. *J. Gen. Physiol.* 101:1–25.

Karplus, M., and G.A. Petsko. 1990. Molecular dynamics simulations in biology. *Nature.* 347:631–639.

Kaupp, U.B., T. Niidome, T. Tanabe, S. Terada, W. Bonigk, W. Stühmer, N.J. Cook, K. Kangawa, H. Matsuo, T. Hirose, et al. 1989. Primary structure and functional expression from complementary DNA of the rod photoreceptor cyclic GMP–gated channel. *Nature.* 342:762–766.

Kaupp, U.B. 1995. Family of cyclic nucleotide gated ion channels. *Curr. Opin. Neurobiol.* 5:434–442.

Kuner, T., L.P. Wollmuth, A. Karlin, P.H. Seeburg, and B. Sakmann. 1996. Structure of the NMDA receptor channel M2 segment inferred from the accessibility of substituted cysteines. *Neuron.* 17: 343–352.

Kurtz, L.L., R.D. Zuhlke, H.-J. Zhang, and R. Joho. 1995. Side-chain accessibilities in the pore of a K^+ channel probed by sulfhydryl-specific reagents after cysteine-scanning mutagenesis. *Biophys. J.* 68:900–905.

Lu, Q., and C. Miller. 1995. Silver as a probe of pore-forming residues in a potassium channel. *Science.* 268:304–307.

Nizzari, M., F. Sesti, M.T. Giraudo, C. Virginio, A. Cattaneo, and V. Torre. 1993. Single-channel properties of cloned cGMP-activated channels from retinal rods. *Proc. R. Soc. Lond. B Biol. Sci.* 254:69–74.

Pascual, J.M., and A. Karlin. 1998. State-dependent accessibility and electrostatic potential in the channel of the acetylcholine receptor. Inferences from rates of reaction of thiosulfonates with substituted cysteines in the M2 segment of the α subunit. *J. Gen. Physiol.* 111:717–739.

Pascual, J.M., C.-C. Shieh, G.E. Kirsch, and A.M. Brown. 1995a. K^+ pore structure revealed by reporter cysteines at inner and outer surfaces. *Neuron.* 14:1055–1063.

Pascual, J.M., C.-C. Shieh, G.E. Kirsch, and A.M. Brown. 1995b. Multiple residues specify external tetraethylammonium blockade in voltage-gated potassium channels. *Biophys. J.* 69:428–434.

Picco, C., and A. Menini. 1993. The permeability of the cGMP-activated channel to organic cations in retinal rods of the tiger salamander. *J. Physiol.* 460:741–758.

Root, M.J., and R. MacKinnon. 1993. Identification of an external divalent cation-binding site in the pore of a cGMP-activated channel. *Neuron.* 11:459–466.

Schrempf, H., O. Schmidt, R. Kummerlen, S. Hinnah, D. Muller, M. Betzler, T. Steinkamp, and R. Wagner. 1995. A prokaryotic potassium ion channel with two predicted transmembrane segments from *Streptomyces lividans. EMBO (Eur. Mol. Biol. Organ.) J.* 14:5170–5178.

Sesti, F., E. Eismann, U.B. Kaupp, M. Nizzari, and V. Torre. 1995. The multi-ion nature of the cGMP-gated channel from vertebrate rods. *J. Physiol.* 487:17–36.

Sesti, F., M. Nizzari, and V. Torre. 1996. Effect of changing temperature on the ionic permeation through the cyclic GMP-gated channel from vertebrate photoreceptors. *Biophys. J.* 70:2616–2639.

Stauffer, D.A., and A. Karlin. 1994. Electrostatic potential of the acetylcholine binding sites in the nicotinic receptor probed by reactions of binding-site cysteines with charged methanethiosulfonates. *Biochemistry.* 33:6840–6849.

Stühmer, W. 1992. Electrophysiological recording from *Xenopus* oocytes. *In* Methods in Enzymology. B. Rudy and L. Iverson, editors. Academic Press, Inc., San Diego, CA. 319–339.

Sun, Z.-P., M.H. Akabas, E.H. Goulding, A. Karlin, and S.A.D. Siegelbaum. 1996. Exposure of residues in the cyclic nucleotide–gated channel pore: P region structure and function in gating. *Neuron.* 16:141–149.

Tempel, B.L., D.M. Papazian, T.L. Schwartz, Y.N. Jan, and L.Y. Jan. 1987. Sequence of a probable potassium channel component encoded at the *Shaker* locus of *Drosophila. Science.* 237:770–775.

Wilson, G.G., and A. Karlin. 1998. The location of the gate in the acetylcholine receptor channel. *Neuron.* 20:1269–1281.

Wolfhart, P., W. Haase, R.S. Molday, and N.J. Cook. 1992. Antibodies against synthetic peptides used to determine the topology and site of glycosylation of the cGMP-gated channel from bovine rod photoreceptors. *J. Biol. Chem.* 267:644–648.

Zagotta, W.N., and S.A. Siegelbaum. 1996. Structure and function of cyclic nucleotide–gated channels. *Annu. Rev. Neurosci.* 19:235–263.